NeuroImage 49 (2010) 1677–1689

Contents lists available at ScienceDirect

NeuroImage

journal homepage: www.elsevier.com/locate/ynimg

Brain networks involved in haptic and visual identification of facial expressions of emotion: An fMRI study

Ryo Kitada [a,*], Ingrid S. Johnsrude [b], Takanori Kochiyama [c], Susan J. Lederman [b]

[a] Division of Cerebral Integration, National Institute for Physiological Sciences, Okazaki, 444-8585, Japan
[b] Department of Psychology, Queen's University, Kingston, Canada K7L 3N6
[c] ATR Brain Activity Imaging Center, Seika-cho 619-0288, Japan

ARTICLE INFO

Article history:
Received 24 April 2009
Revised 10 September 2009
Accepted 12 September 2009
Available online 19 September 2009

ABSTRACT

Previous neurophysiological and neuroimaging studies have shown that a cortical network involving the inferior frontal gyrus (IFG), inferior parietal lobe (IPL) and cortical areas in and around the posterior superior temporal sulcus (pSTS) region is employed in action understanding by vision and audition. However, the brain regions that are involved in action understanding by touch are unknown. Lederman et al. (2007) recently demonstrated that humans can haptically recognize facial expressions of emotion (FEE) surprisingly well. Here, we report a functional magnetic resonance imaging (fMRI) study in which we test the hypothesis that the IFG, IPL and pSTS regions are involved in haptic, as well as visual, FEE identification. Twenty subjects haptically or visually identified facemasks with three different FEEs (disgust, neutral and happiness) and casts of shoes (shoes) of three different types. The left posterior middle temporal gyrus, IPL, IFG and bilateral precentral gyrus were activated by FEE identification relative to that of shoes, regardless of sensory modality. By contrast, an inferomedial part of the left superior parietal lobule was activated by haptic, but not visual, FEE identification. Other brain regions, including the lingual gyrus and superior frontal gyrus, were activated by visual identification of FEEs, relative to haptic identification of FEEs. These results suggest that haptic and visual FEE identification rely on distinct but overlapping neural substrates including the IFG, IPL and pSTS region.

Introduction

A recent study shows that with minimal training humans can haptically recognize facial expressions of emotion (FEE) surprisingly well (Lederman et al., 2007). This result demonstrates that touch can be useful for recognizing the actions of another person. Haptic face recognition may help congenitally blind individuals improve voluntary production of FEEs, which are more poorly recognized than those of sighted individuals (Rinn, 1991; Galati et al., 1997). However, little is known about the neural mechanisms underlying haptic recognition of nonverbal gestures. The present study focused on the neural substrates responsible for haptic recognition of FEEs by sighted individuals.

Previous studies suggest a shared representation for the execution and observation of actions. For instance, the inferior frontal gyrus (IFG) and inferior parietal lobule (IPL) are activated both by imitation and by visual recognition of FEEs (Carr et al., 2003; Montgomery and Haxby, 2008). These results are in accord with other neuroimaging studies suggesting that these regions may constitute the human homologues of the mirror-neuron system (Grafton et al., 1996; Iacoboni et al., 1999; Nishitani and Hari, 2002) in which neurons are activated by both execution and observation of an action (Rizzolatti et al., 1996; Ferrari et al., 2003; Fogassi et al., 2005).

A wealth of neurophysiological studies has shown that cortical areas in and near the superior temporal sulcus (STS region) are sensitive to stimuli that signal the actions of another individual (Perrett et al., 1985; Allison et al., 2000; Haxby et al., 2000). For example, visual recognition of static FEEs activates the posterior STS region (pSTS region) including the middle temporal gyrus (Gorno-Tempini et al., 2001) as well as the superior temporal sulcus (Narumoto et al., 2001). Furthermore, the IFG and STS regions in primates are indirectly connected with each other, via the IPL (Cavada and Goldman-Rakic, 1989; Seltzer and Pandya, 1994). Consequently, it has been proposed that the IFG, IPL and STS regions together constitute a network for action understanding (Rizzolatti et al., 2001).

If the brain network involving the IFG, IPL and STS region is critical for action understanding, such a network should be involved in action understanding, regardless of the sensory modality. Indeed, neurophysiological and neuroimaging studies have shown that the auditory perception of actions also activates IFG and IPL (Kohler et al., 2002; Lahav et al., 2007) and pSTS (Beauchamp et al., 2004) regions. However, to our knowledge, no study has examined whether this brain network contributes to haptic perception of the actions of others.

In the present study, we utilized functional magnetic imaging (fMRI) to test the hypothesis that the IFG, IPL and pSTS regions are

* Corresponding author. Fax: +81 564 55 7786.
E-mail address: kitada@nips.ac.jp (R. Kitada).

1053-8119/$ – see front matter © 2009 Elsevier Inc. All rights reserved.
doi:10.1016/j.neuroimage.2009.09.014

involved in haptic identification of FEEs. On each trial, subjects used either touch or vision to identify one of three emotions (disgust, neutral and happiness) expressed on 3D facemasks, or they identified one of three kinds of 3D casts of (dress shoe, running shoe and hiking boot). We first identify brain regions activated by identification of FEEs relative to identification of shoes in each sensory modality. Then, we tested whether common regions are activated by both sensory modalities. Finally, we examine brain regions involved in haptic and visual identification of specific FEEs.

Materials and methods

Subjects

Twenty healthy volunteers (9 male and 11 female) aged 18–31 years participated in the fMRI study. All participants were right-handed according to the Edinburgh Handedness Inventory (Oldfield, 1971). None of the volunteers had a history of symptoms requiring neurological, psychological or other medical care. All subjects gave written informed consent. The study was approved by the local medical ethics committee at Queen's University (Canada).

Stimuli

We used two different basic-level (Rosch, 1976) classes of objects: plastic casts of faces and shoes (Figs. 1A and 2A). We used shoes as a non-biological object because they are common, complex 3D objects, contain many subordinate-level categories and are similar in size to faces. The facemasks were produced from three female actors (aged 22, 22 and 66 years old), who were trained to generate static facial expressions until a group of four judges agreed that each visual expression portrayed the corresponding emotion (Lederman et al., 2007). The actors' eyes were closed because during manual exploration of live faces, they could be injured. The static facial expressions of the actors were scanned three dimensionally with a color 3D digitizer (3030RGB/PS, Cyberware, Monterey, CA) and printed as plastic casts with a 3D printer (Dimension SST, Stratasys, Inc., Eden Prairie, MN) at Queen's University. Plastic casts of shoes were produced from commercially available shoes using the same procedures. Their size was adjusted to match the size of the facemasks. We prepared three exemplars for each facial emotion (disgust, happiness, neutral) and shoe category (dress, running, hiking). In total, we used 18 exemplars (2 basic levels × 3 subordinate levels × 3 exemplars) in the experiment.

FMRI data acquisition

Functional magnetic resonance images were acquired on a 3-T Siemens Trio whole-body MRI system (Siemens, Erlangen, Germany). Standard sequence parameters were used to obtain the functional images as follows: gradient-echo EPI; repetition time (TR) = 2000 ms; echo time (TE) = 30 ms; flip angle = 78°; 32 axial slices of 3-mm thickness with 25% slice gap; field of view = 192 × 192 mm; and in-plane resolution = 3.0 × 3.0 mm. A single volume approximately covered the whole brain, except for the bottom of the orbitofrontal cortex and cerebellum in larger subjects. A T1-weighted high-resolution anatomical image volume was obtained from each participant (voxel size = 0.9 × 0.9 × 1 mm) before the acquisition of the functional data.

Subjects performed the entire experiment within a single day. In order to discourage them from imagining the objects visually during the task, the haptic-identification task was performed separately and before the visual object-identification task. A 20-min break between

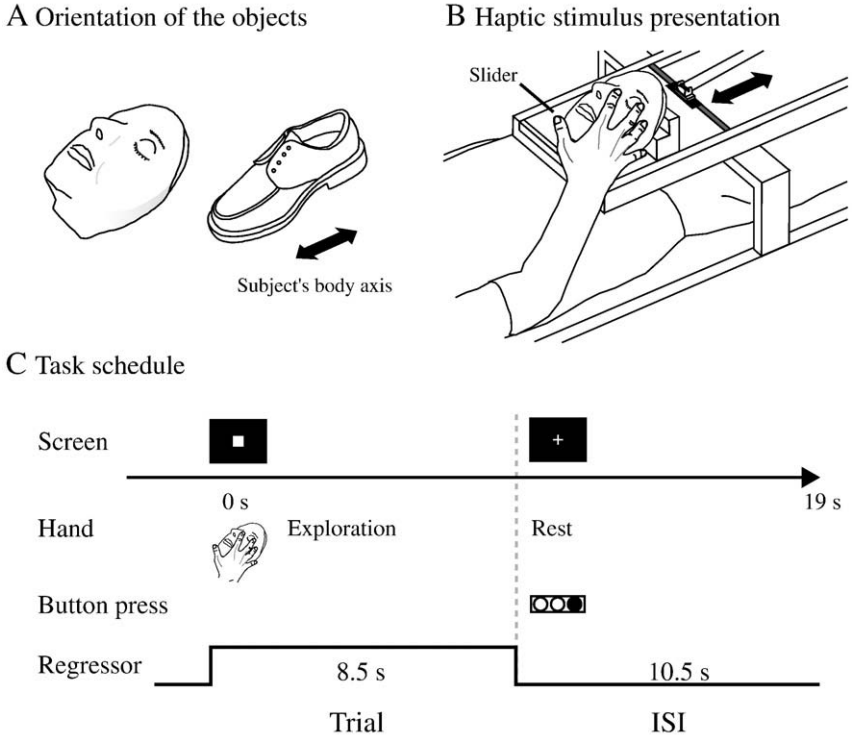

Fig. 1. Haptic task. (A) Two different object categories were used for the experiment: faces (plastic masks) and shoes (plastic casts). Each object category contained three subordinate levels (see also Fig. 2A), with three exemplars per subordinate level (i.e., 18 objects were prepared in total). (B) Each exemplar was mounted on a sheet of Plexiglas moved on a Plexiglas slider. (C) Task schedule. During each trial, subjects were instructed to start exploring the object with their right hand as soon as a white box appeared on the monitor. When the white cross reappeared (i.e., after 8.5-s exploration), subjects were told to stop. They were to respond immediately by using the left hand to press the button corresponding to the numeric code that was appropriate for the subordinate-level category presented. The neural activity during the task block was modeled with a box-car function for each subordinate level of category. The regressor shown in the figure was convolved with a canonical hemodynamic-response function.

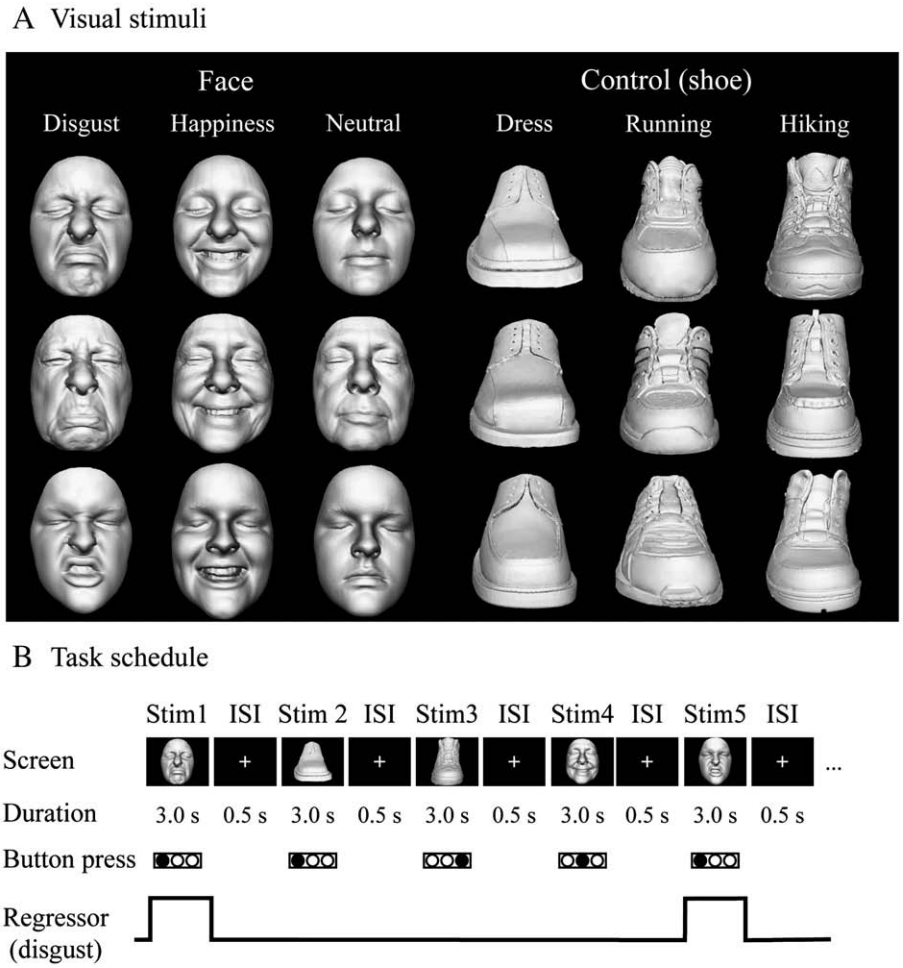

Fig. 2. Visual task. (A) Visual stimuli. A black and white image of each exemplar was used for the task. (B) Task schedule. The subjects were instructed to identify the three subordinate levels for both object categories by pressing one of the three buttons of the response pad with their left hand. The neural activity during the task block was modeled with a box-car function for each subordinate level of category.

the two tasks occurred outside of the scanner. The total experiment lasted ~3 h.

Haptic object-identification task

This task was designed to examine cortical networks involved in *haptic* FEE identification. The subjects were not allowed to see the objects until the final run of the haptic object-identification task was completed.

Haptic stimulus presentation

The subjects lay supine on a bed with their eyes open and their ears plugged and were instructed to relax. They were asked to fixate a white cross on the screen, which they viewed through a mirror over the head coil. A Plexiglas table was placed over the lower half of the body with the front edge at about the level of the abdomen. The stimuli were presented to the subject on the Plexiglas table using a sliding platform (Fig. 1B). The orientation of the presented objects was constrained by physical limitations of the scanning environment; the subjects' hands were somewhat restricted because the distance between the surface of the Plexiglas table and the shell of the bore of the magnet was 19 cm. The orientation of each object class was therefore adjusted so that the subject could comfortably explore each object using one hand (Fig. 1A). The right hand was used to explore the stimuli, while the left arm was extended along the side of the subject's body and the left hand held a response pad.

Each subject completed five runs of the haptic object-identification task (191 volumes per run). A single run consisted of a 342-s task period preceded and followed by 20-s fixation periods. Each of the 18 exemplars was presented once during the task period, for a duration of 8.5 s (Fig. 1C). Object presentations alternated with a 10.5-s inter-stimulus intervals in which subjects made a 3-alternative keypress response to identify the previous object. The order in which the objects were presented in a single run was pseudo-randomized by a genetic algorithm that maximized the estimation efficiency for the tested contrasts (Wager and Nichols, 2003). A software package (Presentation, Neurobehavioral Systems Inc, Albany, CA) was used during the haptic-identification task to present visual cues to the subject and auditory cues via headphones to the experimenter; it was also used to present face and shoe stimuli during the visual-identification task. The auditory cues consisted of a recorded voice that indicated to the experimenter when to present and remove stimuli from the participant.

Task

Before the fMRI experiment, subjects were blindfolded and trained to identify the stimulus objects within 8.5 s and with ≥89% accuracy (equivalent to two mistakes out of 18 exemplars). During training, subjects were asked to identify objects at the subordinate level of categorization (i.e., specific facial expression or shoe type). The same set of objects was used during training and in the fMRI experiment. Participants performed about four trials per object and identified objects with ~96% accuracy in about 6.6 s (on average) during the last

training test. The hand movements used to explore objects were comparable across object categories, consisting mainly of enclosure (i.e., grasp) and contour following (i.e., edge following) exploratory procedures (Lederman and Klatzky, 1987). The training period took less than 30 min.

In each trial, subjects were instructed to start exploring the object as soon as a white box (viewing angle of 0.9°×0.9°) appeared on screen (Fig. 1C). They were asked to cease exploration when the white cross reappeared on screen (i.e., after 8.5 s) and to respond as soon as possible by pressing one of the three buttons on the response pad with the left hand. Each button corresponded to each subordinate-level category for facemasks and shoes. To match the sensorimotor components between object classes, subjects were instructed to carry on exploring the object to confirm their answer if they had already identified the object within 8.5 s. They were also instructed to keep exploration speed constant across the object classes, and when not exploring, to rest that hand upon their chests.

Visual object-identification task

Visual stimulus presentation

A monochromatic image of each exemplar was used for the task (9 images×2 basic-level object categories = 18 images; Fig. 2A). We used frontal images of 3D objects scanned by the same 3D digitizer (3030RGB/PS, Cyberware). The differences in size and perceived brightness of these images were minimized using photo-editing software (Photoshop, Adobe Systems, San Jose, CA). Stimuli were back projected via an LCD projector (LT 265, NEC Viewtechnology, Tokyo, Japan) onto a translucent screen located at the rear of the scanner. The stimuli and the white fixation cross subtended a visual angle of approximately 8.0° and 0.9°, respectively. The subjects' hands extended along the sides of their bodies. The right hand did not touch any object during the visual task, while the left hand held the response pad.

Task

The visual-identification task consisted of five runs (185 volumes per run). A single run consisted of a 315-s task period that was preceded by a 20-s fixation period and followed by a 35-s fixation period. During the task period, each of the 18 exemplars was presented five times. Each image appeared for 3.0 s with an inter-stimulus interval of 0.5 s (3.5 s×90 images = 315 s; Fig. 2B). The relatively long duration was determined by previously published studies on visual identification of emotional facial expressions in which emotion-specific activation was successfully elicited (Phillips et al., 1997, 1998). The order of object presentation within a single run was pseudo-randomized by the design-optimization algorithm used for the haptic task (Wager and Nichols, 2003). Subjects were asked to recognize facial expressions or shoe types by pressing one of the three buttons on the response pad with their left hand. Buttons pressed for the visual task were identical to the buttons pressed in the haptic task. The fMRI experiment was conducted after ~5 min of training, which lasted until subjects reached an accuracy level of ≥89% outside the scanner. The same set of stimuli was used during training and the fMRI experiment.

Data processing

Image processing and statistical analyses were performed using the Statistical Parametric Mapping package (SPM2; Wellcome Department of Cognitive Neurology, London, UK) implemented in MATLAB (Mathworks Inc., Sherborn, MA; Friston et al., 1995a,b). The first five volumes of each fMRI run were discarded to allow the MR signal to reach a state of equilibrium. Functional images from each run were realigned to the first data scan to correct for motion. All functional images and the T1-weighted anatomical images were then co-registered to the first scan of the haptic-identification task. Each co-registered T1-weighted anatomical image was normalized to a standard T1 template image (ICBM 152), which defined the Montreal Neurological Institute (MNI) space. The parameters from this normalization process were then applied to each functional image. The normalized EPI images were spatially filtered using a Gaussian kernel of 8 mm full-width at half maximum (FWHM) in the *x*, *y* and *z* axes.

Statistical analysis

Contrasts between conditions in the haptic and visual object-identification tasks were calculated for individual subjects and incorporated into a random-effects model to make inferences at a population level (Holmes and Friston, 1998).

Initial individual analysis

Two design matrices were prepared for each subject; one comprised five runs of the haptic-identification task and one comprised five runs of the visual-identification task. We fitted a general linear model to the functional MRI data for each subject (Friston et al., 1994; Worsley and Friston, 1995). Neural activity during the trials of both tasks was modeled with box-car functions convolved with the canonical hemodynamic-response function. Each run included six task-related regressors, one for each subordinate-level object category. The time series for each voxel was high-pass filtered at 1/128 Hz. Assuming a first-order autoregressive model, the serial autocorrelation was estimated from the pooled active voxels with the restricted maximum likelihood (ReML) procedure and was used to whiten the data and design matrix (Friston et al., 2002). Motion-related artifacts were minimized by incorporating six parameters (three displacements and three rotations) from the rigid-body realignment stage into each model. Global signal changes were removed by scaling.

In the first-level individual analysis, the estimates for each condition in each individual were compared using linear contrasts. In order to evaluate the neural substrates involved in haptic identification of FEEs, we initially compared the mean activation produced by haptic identification of all FEEs and the mean activation yielded by haptic identification of all shoes in all voxels in the brain (H_{FEE}–H_S). Subsequently, we compared the mean activation produced by visual identification of all FEEs and the mean activation yielded by visual identification of all shoes in all voxels in the brain (V_{FEE}–V_S).

We also evaluated the neural substrates involved in haptic and visual identification of specific FEEs. The contrasts of haptic identification of disgusted faces vs. neutral faces (H_D–H_N) and of haptic identification of happy faces vs. neutral faces (H_H–H_N) were evaluated. Then, the contrasts of visual identification of disgusted faces vs. neutral faces (V_D–V_N) and of visual identification of happy faces vs. neutral faces (V_H–V_N) were evaluated. The resulting set of voxel values for each contrast constituted the SPM{*t*}. The SPM{*t*} was transformed to normal distribution units [SPM{*z*}]. The threshold for SPM{*z*} for the single-subject analyses was set at $Z>3.09$ (equivalent to $p<0.001$ uncorrected for multiple comparisons).

Subsequent group analysis

Contrast images from the individual analyses were used for the group analysis, with between-subjects variance modeled as a random factor. The contrast images obtained from the individual analyses represent the normalized task-related increment of the MR signal of each subject. For each contrast, a one-sample *t* test was performed for every voxel in the brain to obtain population inferences. The resulting set of voxel values for each contrast constituted the SPM{*t*}. The SPM {*t*} was transformed to normal distribution units [SPM{*z*}]. The threshold for SPM{*z*} was set at $Z>3.09$ (equivalent to $p<0.001$ uncorrected). The statistical threshold for the spatial extent test on

the clusters was set at $p<0.05$ and corrected for multiple comparisons over the search volume (Friston et al., 1996).

Search volume for identification of FEEs

We first conducted an analysis for haptic identification of FEEs (H_{FEE}–H_S), in which the search volume was the whole brain (1,449,560 mm^3). Then, since we had an *a priori* hypothesis that the identification of FEEs would activate the IFG, IPL and pSTS regions more than that of shoes, we limited our search to each of these regions, as defined by the probabilistic atlas of Shattuck and colleagues (2008). The search volume for each region was 63,498 mm^3 for bilateral IFG, 99,688 mm^3 for bilateral IPL and 74,464 mm^3 for the bilateral pSTS region (i.e., posterior half of the superior and middle temporal gyri). After this analysis, the same procedure was also conducted for visual identification of FEEs vs. shoes (V_{FEE}–V_S).

Subsequently, in order to test the hypothesis that visual and haptic FEE identification activate common areas, we conducted an analysis for visual activation (V_{FEE}–V_S) within the brain regions activated by (H_{FEE}–H_S). This approach is logically analogous to conjunction analysis (Friston et al., 2005) and has been employed in other studies (e.g., Kitada et al., 2006; Izuma et al., 2008). We limited our search for visual activation to each haptically activated area within the three regions (IFG, IPL and pSTS) as defined by the Shattuck et al. (2008) probabilistic maps. The search volume was 1192 mm^3 for the IFG, 1456 mm^3 for the IPL and 1144 mm^3 for the pSTS region. We also examined whether haptic and visual FEE identification commonly activate regions outside the hypothesized network. The search volume for visual identification of FEEs was defined as all haptically activated regions excluding the three hypothesized regions (8872 mm^3).

Search volume for identification of a specific FEE

We first conducted a whole-brain analysis for each FEE (disgust and happiness) contrasted with neutral faces. Previous studies demonstrated that the anterior insula and basal ganglia are more involved in disgusted faces as compared to other FEEs (Phillips et al., 1997, 1998; Calder et al., 2000). Thus, we subsequently limited our search to bilateral insula and basal ganglia as defined by the probabilistic map (87,600 mm^3) when we evaluated the contrast between haptic identification of disgusted faces vs. neutral faces (H_D–H_N) and the contrast between visual identification of disgusted faces vs. neutral faces (V_D–V_N). In contrast to disgusted faces, we did not set hypothesized regions for happy faces because no consistent pattern of activation has been found in response to happy faces (Posamentier and Abdi, 2003).

Results

Task performance

Haptic object-identification task

Performance accuracy was similar for faces and control objects: 92.3 ± 1.2% (mean ± SEM) for faces and 92.1 ± 1.4% for control objects (Fig. 3). A paired *t* test on performance accuracy comparing faces and control objects showed no significant difference ($p>0.9$). On the other hand, the same test on response time showed that faces produced longer response times than control objects (1090 ± 96 and 1020 ± 89 ms, respectively; $t_{19}=2.73$, $p<0.05$).

Visual object-identification task

Performance accuracy was comparable for faces and control objects: 97.6 ± 0.4% for faces and 96.3 ± 0.8% for control objects (Fig. 3). A paired *t* test on accuracy comparing faces and control objects showed no significant difference ($p>0.05$). However, the same test on response times showed faces produced longer response times than control objects (1099 ± 50 and 1021 ± 44 ms, respectively; $t_{19}=3.46$, $p<0.01$). Collectively, these results show that accuracy for identification of FEEs and control objects was comparable, while response time varied somewhat. Accordingly we will examine whether reliable activation in the brain network for FEEs can be still observed when the difference in RT is included as a covariate that is of no interest in the analysis.

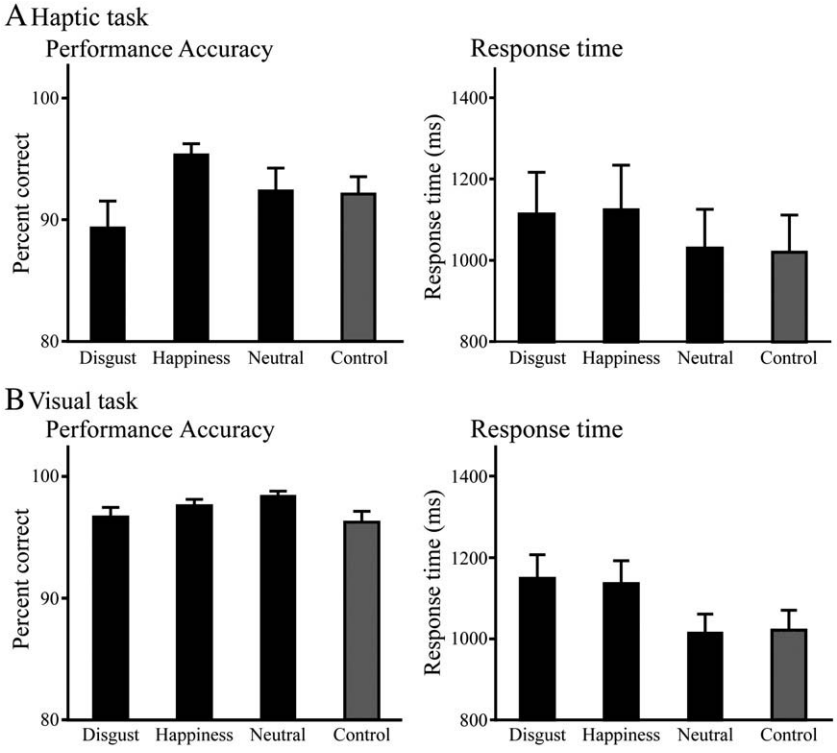

Fig. 3. Behavioral results. These data are presented as the mean ± SEM of 20 subjects.

Task performance among FEEs

Since we are also interested in brain activation related to the perception of disgusted and happy faces relative to neutral FEEs, we further examined task performance among the FEEs.

Haptic object-identification task

One-way ANOVA (three facial expressions) on performance accuracy revealed a significant difference among FEEs ($F_{2,38} = 4.37$, $p < 0.05$) (Fig. 3). Post hoc pairwise comparisons with Sidak–Bonferroni correction showed that happy faces resulted in significantly higher accuracy than disgusted faces ($p < 0.05$). However, the same ANOVA performed on response-time data showed no significant difference ($p > 0.1$).

Visual object-identification task

Although one-way ANOVA (three facial expressions) on accuracy data revealed a significant difference ($F_{2,38} = 3.48$, $p < 0.05$), post hoc pairwise comparisons with Sidak–Bonferroni correction yielded no significant differences ($p > 0.05$). The same ANOVA on response time revealed a significant difference ($F_{3,57} = 13.0$, $p < 0.001$), with post hoc pairwise comparisons showing that disgusted and happy faces took significantly longer to identify than did neutral faces ($ps < 0.01$). Collectively these results reveal that task performance varied among FEEs. However, we will not incorporate these differences into our fMRI analysis because the differences in activation among the FEEs were weak (see below).

fMRI results

A group-average analysis was initially conducted for each sensory modality to identify brain regions activated by identification of FEEs relative to shoes. Subsequently, we tested if common regions within the IFG, IPL and pSTS region were activated by both sensory modalities. Finally, we evaluated neural substrates for specific FEEs (i.e., disgusted and happy faces).

Table 1
Group analyses on identification of FEEs relative to that of shoes.

Cluster size (mm^3)	MNI coordinate			*Z* value	Hem	Anatomical region
	x	*y*	*z*			
Haptics (H_{FEE}–H_S)						
3848	−40	6	54	4.78	L	Middle frontal gyrus
	−46	−6	54	4.49[a]	L	Precentral gyrus
3232	−18	−66	38	4.69	L	Superior parietal lobule
1792	52	2	46	4.69[b]	R	Precentral gyrus
	38	4	60	3.28	R	Middle frontal gyrus
1456	−58	−52	40	3.76	L	Inferior parietal lobule
1192	−46	24	2	3.63[c]	L	Inferior frontal gyrus
1144	−50	−56	6	4.03	L	Middle temporal gyrus
Vision (V_{FEE}–V_S)						
31840	50	−58	12	5.07	R	Middle temporal gyrus
	58	−42	8	5.50	R	Superior temporal gyrus
	52	−46	20	5.86	R	Inferior parietal lobule
	40	−6	−12	3.45	R	Insula
	30	4	−24	4.58	R	Amygdala
	26	−14	−10	4.45	R	Hippocampus
	30	−8	0	4.12	R	Putamen
12224	46	−14	54	4.19	R	Postcentral gyrus
	32	−10	66	4.95[d]	R	Precentral gyrus
	30	2	60	3.63	R	Middle frontal gyrus
	0	2	50	4.50		Superior frontal gyrus
	−6	8	34	3.38	L	Cingulate gyrus
4936	6	−90	−6	5.05	R	Lingual gyrus
	−2	−94	−8	4.78	L	Lingual gyrus
	−16	−100	−6	3.65	L	Middle occipital gyrus
4592	−62	−44	32	5.05	L	Inferior parietal lobule
4440	−54	−60	6	4.70	L	Middle temporal gyrus
	−54	−56	14	4.41	L	Superior temporal gyrus
3968	52	34	−2	5.86[e]	R	Inferior frontal gyrus
3272	12	−50	42	3.94	R	Precuneus
	−56	10	6	3.88[f]	L	Inferior frontal gyrus
	−42	6	−2	3.61	L	Insula
1888	−38	−6	60	3.90[g]	L	Precentral gyrus
	−26	−6	70	4.16	L	Superior frontal gyrus
1320	−36	−2	−22	4.31	L	Inferior temporal gyrus
	−26	2	−14	3.53	L	Amygdala
	−20	−10	−14	3.30	L	Hippocampus
880	−52	30	2	4.13[h]	L	Inferior frontal gyrus

The size of activation was thresholded at $p < 0.05$ corrected for multiple comparisons, when the height threshold was set at $Z > 3.09$; *x*, *y* and *z* are stereotaxic coordinates (mm); Hem, hemisphere; R, right; L, left.

[a–h]Probability values on cytoarchitectonic maps (Amunts et al., 1999; Geyer et al., 1996; Geyer, 2003).

[a] 80% for area 6, 10% for area 1 and 10% for area 4a.

[b] 40% for area 6.

[c] 20% for area 44 and 30% for area 45.

[d] 20% for area 6.

[e] 30% for area 45.

[f] 40% for area 44 and 10% for area 45.

[g] 40% for area 6.

[h] 40% for area 45 and 10% for area 44.

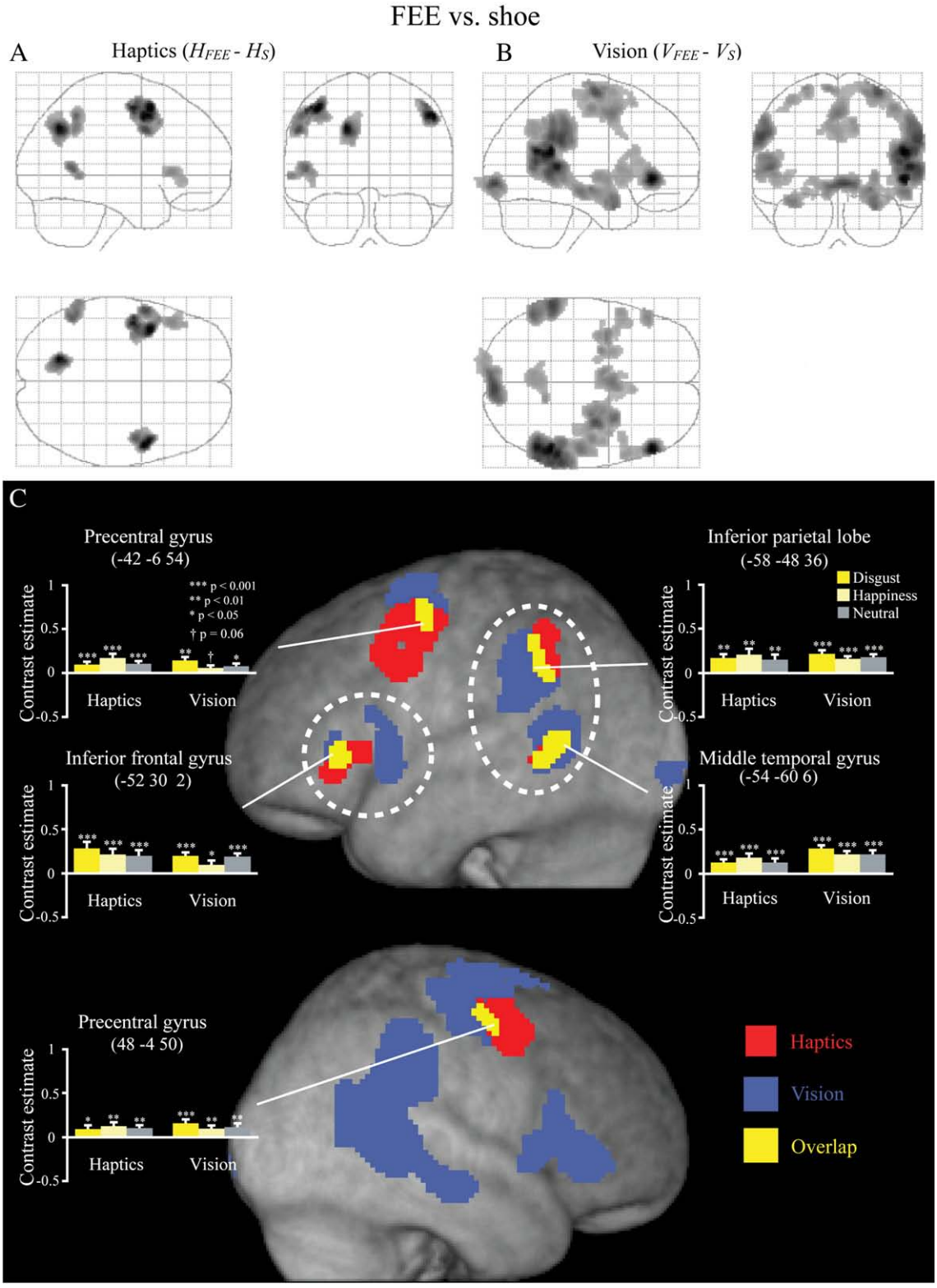

Fig. 4. Brain regions activated by the identification of FEEs (relative to that of shoes). (A, B) Statistical parametric map (SPM) of the average neural activity within the group during the identification of all FEEs compared with that of all shoes. The comparison was performed within each sensory modality. The size of activation was thresholded at $p<0.05$ corrected for multiple comparisons, when the height threshold was set at $Z>3.09$. The 3D information was collapsed into two-dimensional sagittal, coronal and transverse images (i.e., maximum-intensity projections viewed from the right, back and top of the brain). (C) The activation patterns during identification of FEEs relative to shoes were superimposed on a surface-rendered T1-weighted high-resolution MRI averaged across the subjects. A dotted circle around activation indicates activation in the hypothesized regions. Bar graphs indicate contrast estimates for each FEE relative to shoes using a volume of interest with a sphere of 8-mm diameter. The centers of the spheres were the peak coordinates of visual activation. Asterisks indicate the result of one-sample *t* tests. These data are presented as the mean ± SEM of 20 subjects.

Table 2
Group analyses on brain regions activated by visual identification of FEEs (relative to shoes) within regions activated by haptic identification of FEEs (relative to shoes).

Cluster size (mm^3)	MNI coordinate			*Z* value	Hem	Anatomical region	Distance (mm)
	x	*y*	*z*				
944	−54	−60	6	4.70	L	Middle temporal gyrus	5.7
472	−58	−48	36	4.11	L	Inferior parietal lobule	5.7
352	−52	30	2	4.13[a]	L	Inferior frontal gyrus	8.5
264	−42	−6	54	3.43[b]	L	Precentral gyrus	4.0
176	48	−4	50	3.55[c]	R	Precentral gyrus	8.2

The size of activation was thresholded at $p<0.05$ corrected for multiple comparisons, when the height threshold was set at $Z>3.09$; *x*, *y* and *z* are stereotaxic coordinates (mm); Hem, hemisphere; R, right; L, left; Distance, distance between coordinates of peak activation for vision (shown here) and haptics (Table 1).
[a–c]Probability values on cytoarchitectonic maps (Amunts et al., 1999; Geyer et al., 1996; Geyer, 2003).
[a] 40% for area 45 and 10% for area 44.
[b] 70% for area 6, 10% for area 1 and 20% for area 4a.
[c] 60% for area 6.

Haptic identification of FEEs vs. shoes (H_{FEE}–H_S)

Table 1 shows the coordinates of the foci observed for the contrast of haptic identification of FEEs relative to identification of shoes. These included regions of significant activation in the left middle temporal gyrus (pSTS region), left IPL, left superior parietal lobule, left IFG, bilateral precentral gyrus and bilateral middle frontal gyrus (Fig. 4A). Probabilistic cytoarchitectonic maps of Brodmann areas 44 and 45 (Amunts et al., 1999; Eickhoff et al., 2005) revealed that a peak coordinate in the left IFG may be located within area 44 (with a 20% probability) or 45 (with a 30% probability). We also found activation in the right inferior frontal gyrus (MNI coordinates $x=52$, $y=32$, $z=-4$, *Z* value = 4.02, cluster size 320 mm^3; $x=56$, $y=18$, $z=18$, *Z* value = 3.97, 480 mm^3) and pSTS region ($x=60$, $y=-48$, $z=4$, *Z* value = 3.47, 328 mm^3); however, the size of these clusters did not exceed the cluster threshold. We also found weak activation in the left amygdala, which did not exceed the height threshold ($x=-26$, $y=0$, $z=-20$, *Z* value = 2.36).

Probabilistic cytoarchitectonic maps also showed that peak coordinates of activation in the bilateral precentral gyrus were located within area 6 (with ≥40% probability; Geyer, 2003) rather than in the primary motor cortex, area 4 (with ≤10% probability; Geyer et al., 1996). Hence, it is unlikely that activation of the IFG, IPL and middle temporal gyrus in the contrast of FEEs vs. shoes can be explained by quantitative differences in hand movement, which would have resulted in significant activity in the primary motor cortex.

Visual identification of FEEs vs. shoes (V_{FEE}–V_S)

The contrast for the visual identification of FEEs vs. shoes (V_{FEE}–V_S) activated a large network of areas including the hypothesized regions: posterior parts of the superior and middle temporal gyrus, inferior parietal lobule and inferior frontal gyrus bilaterally (Table 1, Fig. 4B). Probabilistic cytoarchitectonic maps (Amunts et al., 1999; Eickhoff et al., 2005) revealed that two peak coordinates in the left IFG may be located within area 44 (with a 40% probability) or 45 (with a 40% probability). A peak coordinate in the right IFG may be located within area 45 (with a 30% probability).

In addition to the areas described above, the contrast for the visual identification of FEEs vs. shoes (V_{FEE}–V_S) produced regions of significant activation in the precuneus, postcentral gyrus, middle frontal gyrus and putamen in the right hemisphere and the middle occipital gyrus, inferior temporal gyrus and cingulate gyrus in the left hemisphere, the lingual gyrus, precentral gyrus, insula, superior frontal gyrus, hippocampus and amygdala bilaterally. The right fusiform gyrus was also activated but the cluster threshold did not reach significance ($x=44$, $y=-48$, $z=-22$, *Z* value = 4.78, 616 mm^3).

Brain regions activated by both haptic and visual FEE identification

As seen in Fig. 4C, we found overlapping activation by haptics and vision within the IFG, IPL, pSTS region and precentral gyrus. In order to statistically test whether haptics and vision activated common regions, the contrast for the visual identification of FEEs vs. shoes (V_{FEE}–V_S) was evaluated within brain regions highlighted by the contrast for the haptic identification of FEEs vs. shoes (H_{FEE}–H_S). This analysis revealed regions of significant activation within the left IFG, left IPL, left middle temporal gyrus and bilateral precentral gyrus (Table 2). As an alternative approach to examining common activation between haptics and vision, we also conducted a conjunction analysis, with the null hypothesis being that one or more of the effects is null (conjunction null hypothesis; Nichols et al., 2005; Friston et al., 2005). This analysis also revealed significant activation in the IFG, IPL and pSTS region (Table S1).

To confirm that similar areas were activated by both haptic and visual identification of FEEs, we examined distances between peak coordinates for the two sensory modalities within each of the commonly activated regions. Within the IFG, IPL and middle temporal gyrus, these distances were less than 10 mm (Table 2). Given that the effective spatial resolution was approximately 12 mm, such small distances are consistent with the notion that the same regions of left

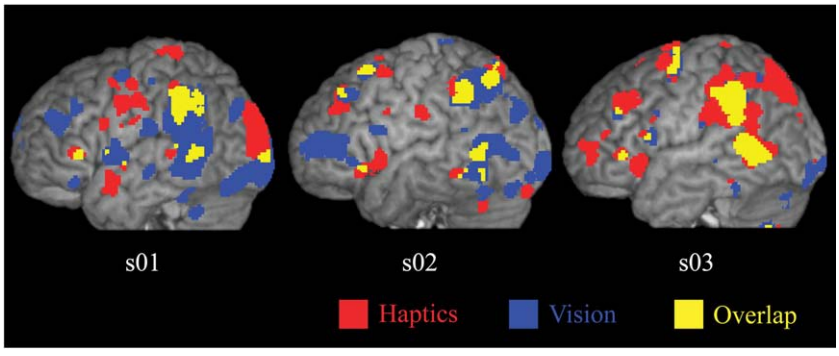

Fig. 5. Individual analysis on brain regions activated by identification of FEEs (relative to that of shoes). The height threshold was set at $Z>3.09$, uncorrected for multiple comparisons. The activation patterns during identification of FEEs relative to shoes were superimposed on a surface-rendered T1-weighted high-resolution MRI of each individual.

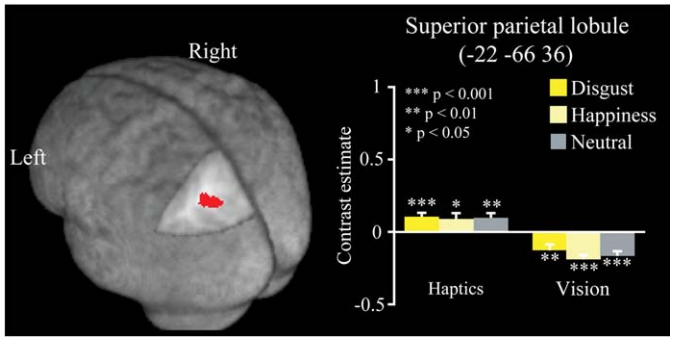

Fig. 6. Brain regions more strongly activated by haptic FEE identification than by visual FEE identification. A paired *t* test of H_{FEE}–H_S and V_{FEE}–V_S was evaluated within the brain regions activated by H_{FEE}–H_S. The size of activation was thresholded at $p<0.05$ corrected for multiple comparisons, when the height threshold was set at $Z>3.09$. Bar graphs indicate activity (contrast estimate) for each FEE relative to shoes using a volume of interest with a sphere of 8-mm diameter. Asterisks indicate the result of one-sample *t* tests. These data are presented as the mean ± SEM of 20 subjects.

IFG, IPL and pSTS region were activated by both haptic and visual identification of FEEs.

In order to confirm that activation in the left IFG, IPL and pSTS region is observed across FEEs, mean contrast estimates were calculated from 8-mm-diameter spheres centered on the peaks (8 mm corresponds to the size of the spatial smoothing kernel applied to these data). One-sample *t* tests on the mean contrast estimates revealed that each FEE showed significantly higher activation than the shoes in each area, regardless of sensory modality (*ps*<0.05, one-tailed; Fig. 4C). This result confirms that the IFG, IPL and pSTS region were activated by all three FEEs. Fig. 5 shows the results of three representative individuals exhibiting activation in the IFG, IPL and pSTS regions during haptic and visual perception of FEEs.

Do differences in response time explain activation in the IFG, IPL and pSTS region?

We found that response time was significantly longer for identification of faces than that of shoes regardless of the sensory modality. In order to confirm that such differences in response time do not explain activation in the IFG, IPL and pSTS region, we conducted the same group analysis as above, but with differences in response time modeled as covariates of no interest (Tables S2 and S3). Bilateral middle temporal gyrus, left IPL and left IFG were also active during haptic and visual identification of FEEs. These results confirm that activation in the IFG, IPL and pSTS regions was not due to a difference in the time taken to respond to FEEs vs. shoes.

Differences in activation patterns elicited by haptic and visual identification of FEEs

We then examined which regions were activated more by haptic identification of FEEs than by visual identification of FEEs (both relative to shoes). The paired *t* test of (H_{FEE}–H_S) and (V_{FEE}–V_S), which was conducted within the brain regions activated by H_{FEE}–H_S, revealed activation in the inferomedial part of the left superior parietal lobule (Fig. 6, Table 3). This region was significantly activated by haptic identification of all FEEs relative to that of shoes, whereas activation in response to visually presented faces was not significantly higher than activation in response to shoes (Fig. 6). Thus, a part of the superior parietal lobule appears to be involved in haptic, but not visual, processing of FEEs.

In order to examine which regions are more activated by visual identification of FEEs as compare to haptic identification of FEEs (both relative to shoes), we also conducted a paired *t* test of (V_{FEE}–V_S) and (H_{FEE}–H_S) within the brain regions activated by (V_{FEE}–V_S) (Table 3). This contrast yielded significant activation in multiple brain regions: bilateral lingual gyrus and superior frontal gyrus, right middle and superior temporal gyrus, IPL and precentral gyrus and left cingulate gyrus. Peak coordinates in the right precentral gyrus and bilateral superior frontal gyrus were probably located within area 6 (with ≥60% probability, Geyer, 2003). None of the regions revealed by this contrast was significantly activated by haptic FEE identification. Even when we lowered the threshold to *Z* value >1.65 (equivalent to $p<0.05$ uncorrected for multiple comparisons), none of the regions except the right pSTS region and right IPL showed activation. Thus, whereas haptic and visual identification of FEEs activated common brain regions including the IFG, IPL and pSTS regions, haptic FEE perception was also associated with activity in other cortical regions that were different for each sensory modality.

Face-related activation in the fusiform gyrus

It is known that haptic object recognition activates the occipito-temporal region (Amedi et al., 2001; James et al., 2002; Pietrini et al., 2004; Zhang et al., 2004). Previous neuroimaging studies have also shown that the haptic recognition of individual faces activates the

Table 3
Group analyses on brain regions more strongly activated by identification of FEEs in one sensory modality than the other.

Cluster size (mm^3)	MNI coordinate			*Z* value	Hem	Anatomical region
	x	*y*	*z*			
(H_{FEE}–H_S)>(V_{FEE}–V_S)						
1056	−22	−66	36	4.13	L	Superior parietal lobule
(V_{FEE}–V_S)>(H_{FEE}–H_S)						
9360	60	−48	−4	4.14	R	Middle temporal gyrus
	60	−36	8	4.44	R	Superior temporal gyrus
	50	−60	18	5.06	R	Inferior parietal lobule
3512	4	−92	−6	5.08	R	Lingual gyrus
	−8	−94	−10	4.07	L	Lingual gyrus
1920	−2	−10	54	4.38[a]	L	Superior frontal gyrus
	4	−8	52	4.37[b]	R	Superior frontal gyrus
	−4	12	32	4.15	L	Cingulate gyrus
1136	26	−10	66	4.53[c]	R	Precentral gyrus
	22	−8	68	4.36[c]	R	Superior frontal gyrus

(H_{FEE}–H_S)>(V_{FEE}–V_S) indicates the result of a paired *t* test of H_{FEE}–H_S and V_{FEE}–V_S evaluated within the brain regions depicted by H_{FEE}–H_S, and (V_{FEE}–V_S)>(H_{FEE}–H_S) indicates the result of a paired *t* test of V_{FEE}–V_S and H_{FEE}–H_S evaluated within the brain regions activated by V_{FEE}–V_S. The size of activation was thresholded at $p<0.05$ corrected for multiple comparisons, when the height threshold was set at $Z>3.09$; *x*, *y* and *z* are stereotaxic coordinates (mm); Hem, hemisphere; R, right; L, left.

[a–d]Probability values on cytoarchitectonic maps.

[a] 60% for area 6 and 10% for area 4a.

[b] 80% for area 6.

[c] 60% for area 6.

fusiform gyrus (Pietrini et al., 2004; Kilgour et al., 2005; James et al., 2006). A recent study specifically demonstrated that the fusiform face area (FFA; Kanwisher et al., 1997) is activated by both haptic and visual face perception (Kitada et al., 2009). That finding is replicated here, in that the FFA was more active during the perception of faces (vs. shoes), regardless of sensory modality (Table S4 and Fig. S1).

Activation specific to an emotional facial expression

Previous studies have shown that visual perception of specific FEEs (e.g., disgusted faces) can activate specific brain regions as compared to other FEEs (Calder et al., 2001; Posamentier and Abdi, 2003). Accordingly, we investigated whether haptic identification of disgusted and happy faces activates the same regions as does visual identification.

Activation specific to disgusted faces (H_D–H_N and V_D–V_N)

We examined whether haptic identification of disgusted faces activates the anterior insula and basal ganglia, regions presumably involved in the visual perception of disgust (Phillips et al., 1997, 1998; Calder et al., 2000). The contrast of disgusted faces vs. neutral faces produced no significant activation in the haptic domain (Table 4), whereas the same contrast of visually presented disgusted faces produced significant activation in the left middle frontal gyrus, in a region adjacent to area 6, according to the probabilistic map of Geyer (2003) (with 10% probability).

When we lowered the threshold to Z value >1.65 (equivalent to $p<0.05$ uncorrected for multiple comparisons), the same contrast in the haptic domain revealed activation in the left anterior insula and basal ganglia (caudate nucleus). The equivalent contrast for vision revealed activation within these same regions (at the threshold of Z value >1.65).

Activation specific to happy faces (H_H–H_N and V_H–V_N)

Unlike the perception of disgusted faces, activation specific to happy faces has not been consistently reported. The contrast of haptic identification of happy vs. neutral faces produced no significant activation. On the other hand, the same contrast for visual conditions produced activation in the left lingual gyrus, right superior parietal lobule, right postcentral gyrus, right precentral gyrus, bilateral cuneus and bilateral middle occipital gyrus.

Discussion

The present study tested the hypothesis that the IFG, IPL and pSTS regions participate in a network that supports haptic and visual FEE identification. Our group-average analysis showed that activity in all of these regions was greater for FEE than for shoe identification, regardless of sensory modality. In addition to these commonalities, activity in some regions depended on sensory modality. An inferomedial part of the superior parietal lobule was activated by haptic, but not visual, FEE identification. Other brain regions including the lingual gyrus and superior frontal gyrus were activated by visual identification of FEEs relative to haptic identification of FEEs. We conclude that haptic and visual identification of FEEs rely on distinct but overlapping neural substrates—the activation of IFG, IPL and pSTS regions is common to both modalities. These commonalities were observed despite the visual and haptic tasks being quite different in form.

Task design

We introduced several differences in the task designs used for haptics and vision (Figs. 1 and 2). Our task design was planned to evaluate not only activation during FEE identification but also activation specific to each FEE (i.e., disgust and happy faces). For this purpose, it was necessary to employ event-related designs for both sensory modalities. Since haptic FEE identification requires a longer trial duration than visual FEE identification, we employed a slow event-related design which resembles a block design. By contrast, the visual task was conducted as a rapid event-related design because subjects could visually identify each FEE very rapidly. Statistical sensitivity of the rapid event-related design is lower than that of the block design (Friston et al., 1999); therefore, we not only maximized the estimation efficiency for the tested contrasts, but also included more repetitions for the visual (cf. haptic) task.

However, these differences in task design should not confound our main finding that common regions were activated by haptic and visual FEE identification, for two reasons. First, these design differences would affect interpretation of activation differences between modalities, but not commonalities. Second, we did not directly compare main effects of modality; rather, we compared

Table 4
Group analyses on disgusted and happy faces relative to neutral face.

Anatomical region	Hem	MNI coordinate			*Z* value	MNI coordinate			*Z* value	Distance (mm)
		x	*y*	*z*		*x*	*y*	*z*		
Disgusted face vs. neutral face										
		Haptics (H_D–H_N)				Vision (V_D–V_N)				
Insula	L	−30	8	−20	3.68*					
	L	−44	6	−10	2.73*	−40	10	−4	2.65*	8.2
Caudate nucleus	L	−10	10	−4	1.81*	−10	8	−4	1.91*	2.0
	R	12	4	2	2.24*					
Putamen	R					26	0	−10	2.07*	
Middle frontal gyrus	L					−28	4	58	4.70[a]	
Happy face vs. neutral face										
		Haptics (H_H–H_N)				Vision (V_H–V_N)				
Lingual gyrus	L					−8	−96	−6	4.36	
Cuneus						0	−102	10	3.41	
Middle occipital gyrus	L					−16	−100	2	4.61	
	R					22	−102	4	5.09	
Superior parietal lobule	R					40	−38	66	3.33	
Postcentral gyrus	R					42	−28	64	4.36	
Precentral gyrus	R					34	−16	68	4.09	

The size of activation was thresholded at $p<0.05$ corrected for multiple comparisons, when the height threshold was set at $Z>3.09$; Hem, hemisphere; R, right; L, left; *x*, *y* and *z* are stereotaxic coordinates (mm); Distance, intermodal distance between coordinates of peak activation.

* Peak of activation, which was not significant and only seen at a lower threshold ($Z>1.65$, equivalent to $p<0.05$ uncorrected for multiple comparisons).

[a] Probability value on cytoarchitectonic maps: 10% for area 6.

task and control activation within each modality. Thus, any effect of repeated presentations or task difficulty is eliminated by directly comparing faces vs. shoes within each sensory modality. It remains possible that one task design may facilitate the observation of activation differences between conditions more than the other (i.e., a possible interaction between task design and object category); regardless, such a difference would not explain why the inferomedial part of the superior parietal lobule showed opposite patterns of activation for haptic and visual FEE identification (Fig. 6). Similarly, it is unlikely that this difference would produce significant activation in multiple brain regions for visual, but not haptic, FEE identification.

Activation of the IFG, IPL and pSTS region in haptic identification of FEEs

In the present study, haptic and visual FEE identification activated brain regions including the IFG, IPL and pSTS regions. Previous studies have shown that these regions are involved in the visual observation of human nonverbal gestures (Grafton et al., 1996; Iacoboni et al., 1999; Gorno-Tempini et al., 2001; Narumoto et al., 2001; Nishitani and Hari, 2002; Carr et al., 2003) and in the auditory perception of another person's actions (Beauchamp et al., 2004; Lahav et al., 2007). Whether these cortical networks are also involved in haptic observation of nonverbal gestures was unclear. Moreover, although previous neuroimaging studies revealed that passive tactile stimulation (relative to rest) can activate the IFG (Hagen et al., 2002), IPL (Numminen et al., 2004; Kitada et al., 2005) and pSTS region (Beauchamp et al., 2008), they have not unequivocally demonstrated the specific aspect of haptic object perception for which these regions are critical. The current study extends the previous ones by showing that a cortical network involving the IFG, IPL and pSTS regions is also involved in the haptic identification of nonverbal gestures, such as FEEs.

It has been proposed that the mirror-neuron system may help an observer understand the actions performed by another individual by causing the observer's motor system to 'resonate' with those actions (Rizzolatti et al., 2001). Previous electromyographic studies have shown that muscles involved in creating emotional facial expressions are also activated when merely observing the faces (Dimberg and Thunberg, 1998; Dimberg et al., 2000). It is possible that our subjects covertly mimicked facial gestures to facilitate FEE recognition. Significant activation for haptic FEE identification was mainly observed in the left hemisphere. It is unlikely that left-hemisphere activation was simply related to naming because this component would have been factored out by the control condition (shoes). Alternatively, it is possible that manual exploration with the right hand enhanced activation of the contralateral (left) hemisphere relative to the ipsilateral (right) hemisphere. It has been suggested that the IFG (Broca's area), IPL and STS regions constitute the human mirror-neuron system (Rizzolatti et al., 2001; Iacoboni and Dapretto, 2006). Although we did not include a task in which subjects express FEEs themselves in order to localize the mirror-neuron system, it is reasonable to speculate that if these three areas participate in the human mirror-neuron system, they would be similarly activated by haptic or visual FEE identification.

We also observed activation in the precentral gyrus (presumably area 6) and middle frontal gyrus for both haptic and visual identification of FEEs. Given that this was observed for both modalities, it cannot simply reflect manual motor activity during haptic exploration. Several previous studies have shown that the dorsal premotor cortex may be involved in visual FEE recognition (Leslie et al., 2004; Grosbras and Paus, 2006). More specifically, passive viewing of dynamic FEEs activates both dorsal and ventral premotor cortex relative to a rest condition (Leslie et al., 2004) and to passive viewing of expanding and contracting circles (Grosbras and Paus, 2006). Hence, it is reasonable to speculate that the precentral gyrus and middle frontal gyrus may work in concert with the IFG, IPL and pSTS region to mediate haptic and visual processing of FEEs.

Activation in identification of specific FEEs

Previous studies showed that the anterior insula and basal ganglia were activated by visual presentation of disgusted faces relative to other FEEs (Phillips et al., 1997, 1998) when subjects performed an implicit (gender-discrimination) task. In the present study, however, only non-significant activation was observed in these regions, regardless of the modality. The main difference between our study and previous studies is that subjects in our study were asked to explicitly recognize FEEs. Explicit recognition of the fearful facial expression reduced expression-specific activity in amygdala relative to a more standard implicit task such as gender discrimination (Critchley et al., 2000; Hariri et al., 2000). Hence, it is possible that explicit recognition of FEEs may not activate these expression-specific regions as strongly as implicit tasks. This speculation may also explain why no significant activation was observed for haptic presentation of happy faces.

Other brain regions involved in haptic and visual identification of FEEs

We observed different patterns of activation for FEE identification between the two sensory modalities. More specifically, an inferomedial part of the superior parietal lobule was activated by haptic, but not visual, FEE identification (both relative to shoes). By contrast, visual identification of FEEs (relative to shoes) activated multiple cortical regions including the bilateral lingual gyrus and superior frontal gyrus more strongly than haptic FEE identification (cf. shoes) (Table 3). In fact, the regions activated by visual identification of FEEs were not activated by haptic identification of FEEs. These results suggest that although the two sensory modalities share a network of cortical areas involved in FEE identification, different regions are additionally engaged by each sensory modality.

Previous studies have shown that an inferomedial part of the superior parietal lobule is involved in haptic and visual spatial processing of objects. For instance, this region is activated by shape perception of 3D objects relative to texture perception of 2D surfaces, regardless of sensory modality (Stilla and Sathian, 2008). The same region is also sensitive to haptic and visual discrimination of object orientation (Sathian et al., 1997; Faillenot et al., 2001; Kaas et al., 2007). Compared to vision, haptic information about objects is typically acquired in a more sequential fashion, especially when the object is larger than the fingertip (Lederman and Klatzky, 1990). Our life-sized objects (faces, shoes) were both fairly large and thus required extensive serial haptic exploration. The inferomedial portion of the superior parietal lobule may contribute to the spatial integration of sequentially obtained inputs. Facemasks – unlike shoes – are not haptically explored or handled on a regular basis (if at all) during daily life. Accordingly, haptic FEE identification may impose greater demands for spatial integration in this brain region (cf. shoes) than corresponding visual identification of FEEs and shoes, both of which are highly familiar and more easily processed on the basis of simultaneous inputs.

On the other hand, a previous fMRI study showed that the lingual gyrus was activated by viewing neutral faces relative to scrambled images (Kesler-West et al., 2001). Compared to haptics, vision can extract spatial features of FEEs simultaneously. Thus, activation of this region may reflect such characteristics in visual processing of FEEs. In addition, another previous fMRI study revealed that the superior frontal gyrus was strongly activated by imitation of FEEs but only weakly activated by visual observation of FEEs (both relative to a rest condition) (Leslie et al., 2004). Since this region corresponds to the supplementary motor area (SMA), it is possible that simultaneous

input of vision may recruit the additional motor system to 'resonate' for understanding FEEs.

In conclusion, the present study demonstrates that haptic and visual FEE identification commonly activate left IFG, IPL and pSTS regions. By contrast, we also observed a difference in activation patterns between the two modalities. An inferior portion of the superior parietal lobule was solely activated by haptic FEE identification (cf. shoes). In contrast, visual FEE identification activated multiple cortical regions (including the bilateral lingual gyrus) more strongly than haptic FEE identification (cf. shoes). Hence, we conclude that haptic and visual FEE identification rely on distinct but overlapping neural substrates including the IFG, IPL and pSTS region.

Acknowledgments

This study was supported by a Postdoctoral Fellowship for Research Abroad from the Japan Society for the Promotion of Science and a Grant-in-Aid for Scientific Research on Innovative Areas, "Face perception and recognition" (21119524) from the Ministry of Education, Science, Sports and Culture, Japan, to R.K. and grants from the Natural Sciences and Engineering Research Council of Canada and the Canadian Institutes of Health Research to S.L. We thank S. David for assistance with neuroimaging, C. Hamilton for technical assistance, W. Sato for his valuable advice on this project and N. Sadato for his valuable comments on an earlier manuscript.

Appendix A. Supplementary data

Supplementary data associated with this article can be found, in the online version, at doi:10.1016/j.neuroimage.2009.09.014.

References

Allison, T., Puce, A., McCarthy, G., 2000. Social perception from visual cues: role of the STS region. Trends Cogn. Sci. 4, 267–278.
Amedi, A., Malach, R., Hendler, T., Peled, S., Zohary, E., 2001. Visuo-haptic object-related activation in the ventral visual pathway. Nat. Neurosci. 4, 324–330.
Amunts, K., Schleicher, A., Burgel, U., Mohlberg, H., Uylings, H.B., Zilles, K., 1999. Broca's region revisited: cytoarchitecture and intersubject variability. J. Comp. Neurol. 412, 319–341.
Beauchamp, M.S., Argall, B.D., Bodurka, J., Duyn, J.H., Martin, A., 2004. Unraveling multisensory integration: patchy organization within human STS multisensory cortex. Nat. Neurosci. 7, 1190–1192.
Beauchamp, M.S., Yasar, N.E., Frye, R.E., Ro, T., 2008. Touch, sound and vision in human superior temporal sulcus. NeuroImage 41, 1011–1020.
Calder, A.J., Keane, J., Manes, F., Antoun, N., Young, A.W., 2000. Impaired recognition and experience of disgust following brain injury. Nat. Neurosci. 3, 1077–1078.
Calder, A.J., Lawrence, A.D., Young, A.W., 2001. Neuropsychology of fear and loathing. Nat. Rev. Neurosci. 2, 352–363.
Carr, L., Iacoboni, M., Dubeau, M.C., Mazziotta, J.C., Lenzi, G.L., 2003. Neural mechanisms of empathy in humans: a relay from neural systems for imitation to limbic areas. Proc. Natl. Acad. Sci. U. S. A. 100, 5497–5502.
Cavada, C., Goldman-Rakic, P.S., 1989. Posterior parietal cortex in rhesus monkey: II. Evidence for segregated corticocortical networks linking sensory and limbic areas with the frontal lobe. J. Comp. Neurol. 287, 422–445.
Critchley, H., Daly, E., Phillips, M., Brammer, M., Bullmore, E., Williams, S., Van Amelsvoort, T., Robertson, D., David, A., Murphy, D., 2000. Explicit and implicit neural mechanisms for processing of social information from facial expressions: a functional magnetic resonance imaging study. Hum. Brain Mapp. 9, 93–105.
Dimberg, U., Thunberg, M., 1998. Rapid facial reactions to emotional facial expressions. Scand. J. Psychol. 39, 39–45.
Dimberg, U., Thunberg, M., Elmehed, K., 2000. Unconscious facial reactions to emotional facial expressions. Psychol. Sci. 11, 86–89.
Eickhoff, S.B., Stephan, K.E., Mohlberg, H., Grefkes, C., Fink, G.R., Amunts, K., Zilles, K., 2005. A new SPM toolbox for combining probabilistic cytoarchitectonic maps and functional imaging data. NeuroImage 25, 1325–1335.
Faillenot, I., Sunaert, S., Van Hecke, P., Orban, G.A., 2001. Orientation discrimination of objects and gratings compared: an fMRI study. Eur. J. Neurosci. 13, 585–596.
Ferrari, P.F., Gallese, V., Rizzolatti, G., Fogassi, L., 2003. Mirror neurons responding to the observation of ingestive and communicative mouth actions in the monkey ventral premotor cortex. Eur. J. Neurosci. 17, 1703–1714.
Fogassi, L., Ferrari, P.F., Gesierich, B., Rozzi, S., Chersi, F., Rizzolatti, G., 2005. Parietal lobe: from action organization to intention understanding. Science 303, 662–667.
Friston, K.J., Jezzard, P., Turner, R., 1994. Analysis of functional MRI time-series. Hum. Brain Mapp. 1, 153–171.
Friston, K.J., Ashburner, J., Frith, C.D., Heather, J.D., Frackowiak, R.S.J., 1995a. Spatial registration and normalization of images. Hum. Brain Mapp. 2, 165–188.
Friston, K.J., Holmes, A.P., Worsley, K.J., Poline, J.B., Frith, C.D., Frackowiak, R.S.J., 1995b. Statistical parametric maps in functional imaging: a general linear approach. Hum. Brain Mapp. 2, 189–210.
Friston, K.J., Holmes, A., Poline, J.B., Price, C.J., Frith, C.D., 1996. Detecting activations in PET and fMRI: levels of inference and power. NeuroImage 4, 223–235.
Friston, K.J., Zarahn, E., Josephs, O., Henson, R.N., Dale, A.M., 1999. Stochastic designs in event-related fMRI. NeuroImage 10, 607–619.
Friston, K.J., Glaser, D.E., Henson, R.N., Kiebel, S., Phillips, C., Ashburner, J., 2002. Classical and Bayesian inference in neuroimaging: applications. NeuroImage 16, 484–512.
Friston, K.J., Penny, W.D., Glaser, D.E., 2005. Conjunction revisited. NeuroImage 25, 661–667.
Galati, D., Scherer, K.R., Ricci-Bitti, P.E., 1997. Voluntary facial expression of emotion: comparing congenitally blind with normally sighted encoders. J. Pers. Soc. Psychol. 73, 1363–1379.
Geyer, S., 2003. The Microstructural Border between the Motor and the Cognitive Domain in the Human Cerebral Cortex. Springer Press, Wien.
Geyer, S., Ledberg, A., Schleicher, A., Kinomura, S., Schormann, T., Bürgel, U., Klingberg, T., Larsson, J., Zilles, K., Roland, P.E., 1996. Two different areas within the primary motor cortex of man. Nature 382, 805–807.
Gorno-Tempini, M.L., Pradelli, S., Serafini, M., Pagnoni, G., Baraldi, P., Porro, C., Nicoletti, R., Umità, C., Nichelli, P., 2001. Explicit and incidental facial expression processing: an fMRI study. NeuroImage 14, 465–473.
Grafton, S.T., Arbib, M.A., Fadiga, L., Rizzolatti, G., 1996. Localization of grasp representations in humans by positron emission tomography 2. Observation compared with imagination. Exp. Brain Res. 112, 103–111.
Grosbras, M.H., Paus, T., 2006. Brain networks involved in viewing angry hands or faces. Cereb. Cortex 16, 1087–1096.
Hagen, M.C., Zald, D.H., Thornton, T.A., Pardo, J.V., 2002. Somatosensory processing in the human inferior prefrontal cortex. J. Neurophysiol. 88, 1400–1406.
Hariri, A.R., Bookheimer, S.Y., Mazziotta, J.C., 2000. Modulating emotional responses: effects of a neocortical network on the limbic system. NeuroReport 11, 43–48.
Haxby, J.V., Hoffman, E.A., Gobbini, M.I., 2000. The distributed human neural system for face perception. Trends Cogn. Sci. 4, 223–233.
Holmes, A.P., Friston, K.J., 1998. Generalisability, random effects and population inference. NeuroImage 7, S754.
Iacoboni, M., Dapretto, M., 2006. The mirror neuron system and the consequences of its dysfunction. Nat. Rev. Neurosci. 7, 942–951.
Iacoboni, M., Woods, R.P., Brass, M., Bekkering, H., Mazziotta, J.C., Rizzolatti, G., 1999. Cortical mechanisms of human imitation. Science 286, 2526–2528.
Izuma, K., Saito, D.N., Sadato, N., 2008. Processing of social and monetary rewards in the human striatum. Neuron 58, 284–294.
James, T.W., Humphrey, G.K., Gati, J.S., Servos, P., Menon, R.S., Goodale, M.A., 2002. Haptic study of three-dimensional objects activates extrastriate visual areas. Neuropsychologia 40, 1706–1714.
James, T.W., Servos, P., Kilgour, A.R., Huh, E., Lederman, S., 2006. The influence of familiarity on brain activation during haptic exploration of 3-D facemasks. Neurosci. Lett. 397, 269–273.
Kaas, A.L., van Mier, H., Goebel, R., 2007. The neural correlates of human working memory for haptically explored object orientations. Cereb. Cortex 17, 1637–1649.
Kanwisher, N., McDermott, J., Chun, M.M., 1997. The fusiform face area: a module in human extrastriate cortex specialized for face perception. J. Neurosci. 17, 4302–4311.
Kesler-West, M.L., Andersen, A.H., Smith, C.D., Avison, M.J., Davis, C.E., Kryscio, R.J., Blonder, L.X., 2001. Neural substrates of facial emotion processing using fMRI. Brain Res. Cogn. Brain Res. 11, 213–226.
Kilgour, A.R., Kitada, R., Servos, P., James, T.W., Lederman, S.J., 2005. Haptic face identification activates ventral occipital and temporal areas: an fMRI study. Brain Cogn. 59, 246–257.
Kitada, R., Hashimoto, T., Kochiyama, T., Kito, T., Okada, T., Matsumura, M., Lederman, S.J., Sadato, N., 2005. Tactile estimation of the roughness of gratings yields a graded response in the human brain: an fMRI study. NeuroImage 25, 90–100.
Kitada, R., Kito, T., Saito, D.N., Kochiyama, T., Matsumura, M., Sadato, N., Lederman, S.J., 2006. Multisensory activation of the intraparietal area when classifying grating orientation: a functional magnetic resonance imaging study. J. Neurosci. 26, 7491–7501.
Kitada, R., Johnsrude, I.S., Kochiyama, T., Lederman, S.J., 2009. Functional specialization and convergence in the occipito-temporal cortex supporting haptic and visual identification of human faces and body parts: an fMRI study. J. Cogn. Neurosci. 21, 2027–2045.
Kohler, E., Keysers, C., Umiltà, M.A., Fogassi, L., Gallese, V., Rizzolatti, G., 2002. Hearing sounds, understanding actions: action representation in mirror neurons. Science 297, 846–848.
Lahav, A., Saltzman, E., Schlaug, G., 2007. Action representation of sound: audiomotor recognition network while listening to newly acquired actions. J. Neurosci. 27, 308–314.
Lederman, S.J., Klatzky, R.L., 1987. Hand movements: a window into haptic object recognition. Cogn. Psychol. 19, 342–368.
Lederman, S.J., Klatzky, R.L., 1990. Haptic identification of common objects: knowledge-driven exploration. Cogn. Psychol. 22, 421–459.
Lederman, S.J., Klatzky, R.L., Abramowicz, A., Salsman, K., Kitada, R., Hamilton, C., 2007. Haptic recognition of static and dynamic expressions of emotion in the live face. Psychol. Sci. 18, 158–164.
Leslie, K.R., Johnson-Frey, S.H., Grafton, S.T., 2004. Functional imaging of face and hand imitation: towards a motor theory of empathy. NeuroImage 21, 601–607.

Montgomery, K.J., Haxby, J.V., 2008. Mirror neuron system differentially activated by facial expressions and social hand gestures: a functional magnetic resonance imaging study. J. Cogn. Neurosci. 20, 1866–1877.
Narumoto, J., Okada, T., Sadato, N., Fukui, K., Yonekura, Y., 2001. Attention to emotion modulates fMRI activity in human right superior temporal sulcus. Brain Res. Cogn. Brain Res. 12, 225–231.
Nichols, T., Brett, M., Andersson, J., Wager, T., Poline, J.B., 2005. Valid conjunction inference with the minimum statistic. NeuroImage 25, 653–660.
Nishitani, N., Hari, R., 2002. Viewing lip forms: cortical dynamics. Neuron 36, 1211–1220.
Numminen, J., Schürmann, M., Hiltunen, J., Joensuu, R., Jousmäki, V., Koskinen, S.K., Salmelin, R., Hari, R., 2004. Cortical activation during a spatiotemporal tactile comparison task. NeuroImage 22, 815–821.
Oldfield, R.C., 1971. The assessment and analysis of handedness: The Edinburgh Inventory. Neuropsychologia 9, 97–113.
Perrett, D.I., Smith, P.A., Potter, D.D., Mistlin, A.J., Head, A.S., Milner, A.D., Jeeves, M.A., 1985. Visual cells in the temporal cortex sensitive to face view and gaze direction. Proc. R. Soc. Lond., B Biol. Sci. 223, 293–317.
Phillips, M.L., Young, A.W., Senior, C., Brammer, M., Andrew, C., Calder, A.J., Bullmore, E. T., Perrett, D.I., Rowland, D., Williams, S.C., Gray, J.A., David, A.S., 1997. A specific neural substrate for perceiving facial expressions of disgust. Nature 389, 495–498.
Phillips, M.L., Young, A.W., Scott, S.K., Calder, A.J., Andrew, C., Giampietro, V., Williams, S.C., Bullmore, E.T., Brammer, M., Gray, J.A., 1998. Neural responses to facial and vocal expressions of fear and disgust. Proc. Biol. Sci. 265, 1809–1817.
Pietrini, P., Furey, M.L., Ricciardi, E., Gobbini, M.I., Wu, W.H., Cohen, L., Guazzelli, M., Haxby, J.V., 2004. Beyond sensory images: object-based representation in the human ventral pathway. Proc. Natl. Acad. Sci. U. S. A. 101, 5658–5663.
Posamentier, M.T., Abdi, H., 2003. Processing faces and facial expressions. Neuropsychol. Rev. 13, 113–143.
Rinn, W., 1991. Neuropsychology of facial expression. In: Feldman, RS, Rimé, B (Eds.), Fundamentals of Nonverbal Behavior. Cambridge University Press, New York, pp. 3–29.
Rizzolatti, G., Fadiga, L., Gallese, V., Fogassi, L., 1996. Premotor cortex and the recognition of motor actions. Brain Res. Cogn. Brain Res. 3, 131–141.
Rizzolatti, G., Fogassi, L., Gallese, V., 2001. Neurophysiological mechanisms underlying the understanding and imitation of action. Nat. Rev. Neurosci. 2, 661–670.
Rosch, E.H., 1976. Basic objects in natural categories. Cogn. Psychol. 8, 382–439.
Sathian, K., Zangaladze, A., Hoffman, J.M., Grafton, S.T., 1997. Feeling with the mind's eye. NeuroReport 8, 3877–3881.
Seltzer, B., Pandya, D.N., 1994. Parietal, temporal, and occipital projections to cortex of the superior temporal sulcus in the rhesus monkey: a retrograde tracer study. J. Comp. Neurol. 343, 445–463.
Shattuck, D.W., Mirza, M., Adisetiyo, V., Hojatkashani, C., Salamon, G., Narr, K.L., Poldrack, R.A., Bilder, R.M., Toga, A.W., 2008. Construction of a 3D probabilistic atlas of human cortical structures. NeuroImage 39, 1064–1080.
Stilla, R., Sathian, K., 2008. Selective visuo-haptic processing of shape and texture. Hum. Brain Mapp. 29, 1123–1138.
Wager, T.D., Nichols, T.E., 2003. Optimization of experimental design in fMRI: a general framework using a genetic algorithm. NeuroImage 18, 293–309.
Worsley, K.J., Friston, K.J., 1995. Analysis of fMRI time-series revisited—again. NeuroImage 2, 173–181.
Zhang, M., Weisser, V.D., Stilla, R., Prather, S.C., Sathian, K., 2004. Multisensory cortical processing of object shape and its relation to mental imagery. Cogn. Affect. Behav. Neurosci. 4, 251–259.